DTU Library

CFD Simulations of the Mexico Wind Tunnel and Wind Turbine

Réthoré, Pierre-Elouan Mikael; Zahle, Frederik; Sørensen, Niels N.; Bechmann, Andreas

Published in:
Proceedings

Publication date:
2011

Document Version
Publisher's PDF, also known as Version of record

CFD model of the MEXICO wind tunnel

P.-E. Réthoré*, N. N. Sørensen, F. Zahle, A. Bechmann and H. A. Madsen
Wind Energy Division, Risø DTU, DK-4000 Roskilde, Denmark.
* pire@risoe.dtu.dk. tel: +45 21331293.

Abstract

The MEXICO Experiment is reproduced in CFD, including the geometry of the wind tunnel and the wind turbine rotor. The wind turbine is modelled both as a full rotor and as an actuator disc. Various questions regarding the wind tunnel effects on the measurements are investigated. As in a previous work carried out without modelling the wind tunnel, the CFD methods are found to give satisfying agreement with the axial velocity deficit in the wake. However, confirming the previous work, the blade loadings estimated from CFD are found to be consistently larger than the one estimated from measurements. In order to investigate further this issue, the loadings estimated from measurement are used with an actuator disc model. This approach gives a too small wake deficit in comparison with the measurements, which tends to agree with the full rotor computation results.

1 Introduction

The EU FP5 project 'Model EXperiments In COntrolled COnditions' or 'MEXICO' [13] was a wind tunnel experiment campaign leaded by the Energy research Center of the Netherland (ECN). A 4.5 m diameter fully instrumented wind turbine was set up in the 9.5×9.5 m open jet wind tunnel of the German Dutch Wind tunnel Organization (DNW). Some 'breathing slots' were introduced behind the collector to avoid flow recirculation. The forces acting on the blades were estimated using pressure sensors at 5 sections on the blades. The flow upstream and downstream of the wind turbine was observed using Particle Image Velocimetry (PIV). The purpose of this experiment was to provide high quality experimental data to validate various types of wind turbine models. An exhaustive literature list concerning the experiment and the related analysis is available on the MEXICO Experiment website [1].

Risø DTU has developed a set of Wind Energy CFD tools to model the flow passing through wind turbines [9, 15] or in complex terrain [2, 14]. Risø DTU has therefore been interested from the beginning to participate in the MEXICO Experiment in order to compare the measurements with our different models.

When dealing with new types of wind tunnel experiments many questions arise on the possible unexpected influence of the wind tunnel on the measurements. Some of the questions addressed in this study are as follow. How far downstream and upstream of the wind turbine is the flow unaffected by the wind tunnel geometry? Do the 'breathing slots' have a noticeable influence on the measurements? Is the flow influenced by the wind tunnel room geometry? In order to investigate those questions the geometry of the DWN wind tunnel is used as a background mesh to the CFD computation.

Moreover, previous CFD Full Rotor (FR) calculations where done by Bechmann et al. [3] on the MEXICO wind turbine rotor, without considering the wind tunnel. These results show that it is possible to obtain a satisfying fit with the flow measurements, while at the same time to have loadings on the wind turbine blades that are significantly larger than what the measurements predict. This could potentially indicate that the estimation of the wind turbine blade loading have been underestimated during the experiments. The Actuator Disc (AD) method [12], which takes the loadings from the MEXICO experiment, is used in this work to investigate this issue.

The rest of the paper is organized as follow. First, a brief description of the different methods used in this work. Then, the presentation of different test cases run and associated results. Finally, a discussion of different issues such as the wind tunnel Reynolds Number independence, the flow asymmetry, the wind tunnel perturbations, the influence of the breathing slots and of the jet oscillation. Finally, the mismatch between blade loadings and flow features is addressed.

2 Method

2.1 Flow Solver

The flow solver used in this work, EllipSys, is an in-house general purpose CFD code developed at Risø DTU [14] and DTU MEK [7]. It is a flow solver based on a finite-volume spatial and temporal discretization of the incompressible Navier-Stokes Equations formulated in general curvilinear coordinates. The variables are collocated in the cell centers to enable computations using complex geometrical meshes. The pressure correction method is based on the Rhie-Chow algorithm, which is modified for the treatment of the body forces of the actuator disc model [10] and is accelerated using a multigrid technique. The flow is solved successively over three levels of discretization in order to accelerate the convergence and to ensure a grid independent solution [7]. The equations can be discretized using different schemes (see Section 2.3 & 2.4). For the full rotor computation, the PISO [4] method is used to solve the Navier-Stokes Equations system, while for the actuator disc method, the SIMPLE [8] method is used. The flow equations are discretized using a QUICK formulation [5] in both methods. The Reynolds stresses are modelled in the Navier-Stokes equations using the eddy-viscosity assumption and a k-ω-SST [6] turbulence model.

2.2 Wind Tunnel Mesh

Most of the human work time of this project was spent on meshing the DWN wind tunnel. The shape of the nozzle and collector are confidential and a Non Disclosure Agreement was signed with DWN in order to obtain them. In order to be able to freely publish the results the decision was made to not show the final shapes of the nozzle and collectors. All the figures illustrating those parts are therefore whether slightly altered, obstructed or a free 'artistic' representation (done prior to

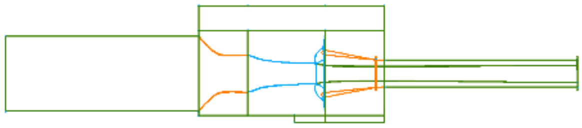

Figure 1: Horizontal view of the mesh blocks.

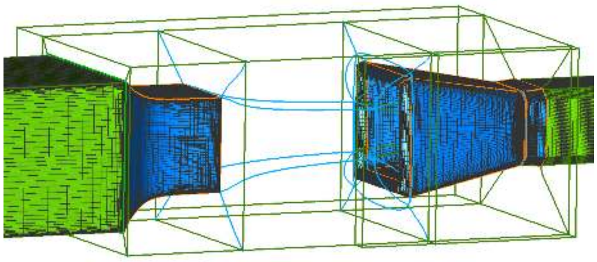

Figure 2: Perspective view of the mesh blocks.

obtaining the confidential information), and should not be considered as realistic in any way. The simulations are, however, carried out using the complete nozzle and collector shapes.

The wind tunnel is meshed using the software PointWise as 386 32^3-cell structured blocks (around 12M cells). The support structure of the wind turbine rotor, as well as the support structure of the collector are not considered in this study. These structures are rather large blunt bodies, and should have an important impact on the flow behavior around these regions. It is therefore assumed that the region of interest and the overall loads on the wind turbine blade are not influenced by these support structures. Some details of the mesh structure are illustrated on Fig.1-3. Note that in these figures the blocks illustrated have not yet been subdivided into 32^3-cell elements.

The inlet and outlet of the domain are extended, and the cells size are gradually stretched, expanding towards the inlet and outlet (see Fig.1). This is done in order to avoid to have some influence from the boundary condition over the zone of interest, and to enforce a numerical dissipation to avoid flow structures to create unstability while passing the outlet. As these regions are nowhere near the interesting locations their geometry should have little influence on the results.

The wall boundary conditions are taken as

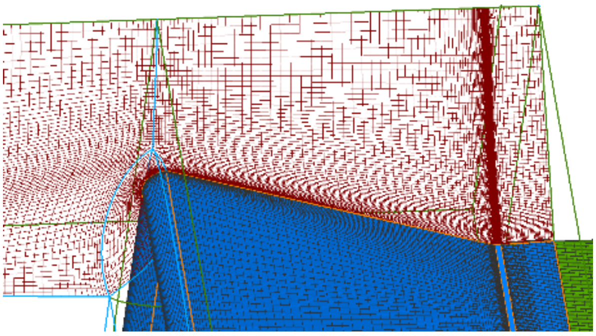

Figure 3: Detail of the collector lips meshing. The 'breathing slots' are visible on the right side of the mesh.

slip condition (symmetry). This is done to avoid resolving the boundary layer at the wall surface for speeding up both the meshing and computational expenses. The shortcoming of this approach is that there is not any development of a boundary layer on the walls of the room, nozzle and collector. The assumption made is therefore that this boundary layer does not influence the region of the flow where the measurements are made.

The "breathing slots" located at the exit of the collector are taken into account in the mesh geometry (see Fig.3). In order to assess their effect, a variation of the wind tunnel mesh is done without the slots (referred later as "WT-no hole").

2.3 Full Rotor Computation

In a previous work by Bechmann et al., the wind turbine rotor was mesh with an o-geometry. For an in-depth description of the method used to mesh the surface of the rotor and compute the MEXICO rotor, without wind tunnel, see [3].

In the current work, the full geometry of the MEXICO wind turbine rotor, excluding the spinner, hub, tower and support structured, is meshed and is added to the wind tunnel mesh through an overset grid methodology [15]. Note that the surface mesh of the rotor is the same as used in [3]. Three overset meshes are used in addition to the wind tunnel to smoothly interpolate from the very fine rotor mesh to the coarser background mesh (see Fig.4. One cylindrical mesh close to the turbine that rotates with the rotor mesh, and one coarser, which is fixed relative to the wind tunnel mesh and extends up to one rotor diameter downstream. In the case of the mesh without wind tunnel, a Cartesian background mesh is used

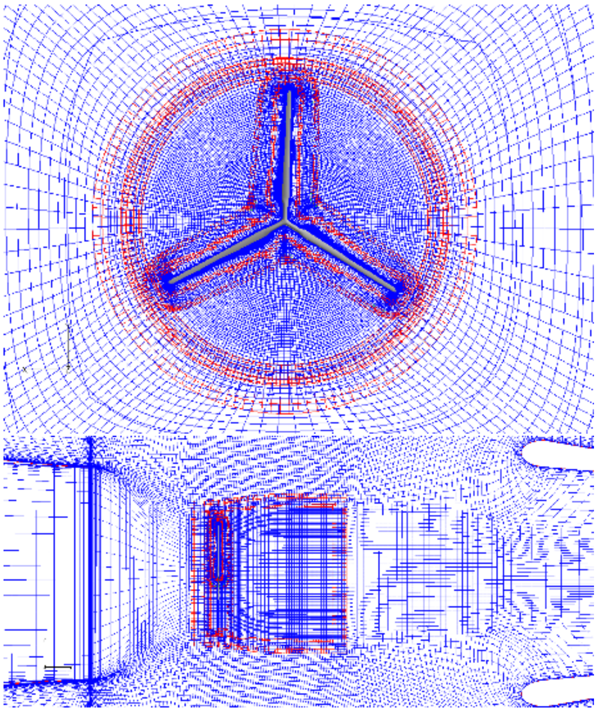

Figure 4: Detail of the full rotor computation mesh. top: front view. bottom: side view.

instead of the wind tunnel mesh. The rotor mesh is designed to have a maximum cell size at the blade surface so that $y^+ < 2$. The total mesh composed of the background wind tunnel mesh described in the previous section and the three successive refinement meshes represents in total 798 32^3-cell blocks (26M+ cells). The code runs in transient mode at 7.5 hours per revolution on 160 CPUs. The result shown are run for 10 revolutions, so 3.2 days.

Fig.5 illustrates the full rotor computation of the MEXICO rotor in the DWN wind tunnel.

2.4 Actuator Disc Model

The actuator disc model [12] is spreading the blade forces over a disc and applying them into the wind tunnel background mesh. The forces are treated in a special way to avoid pressure-velocity decoupling [10]. In all the actuator disc simulations, the forces are splined from the 5 wind turbine blade pressure sensor measurements (see Fig.6).

Two types of solutions are considered, an unsteady Detached Eddy Simulation (DES) solution

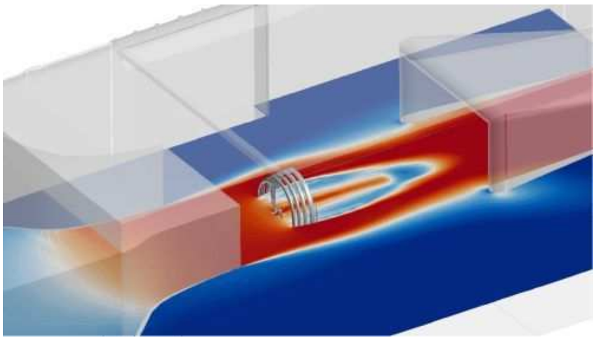

Figure 5: Full rotor computation of the MEXICO rotor in the DWN wind tunnel. Vorticity iso-surface and axis velocity colour contour in an horizontal plane at hub height. The wind tunnel geometry is visible in transparent.

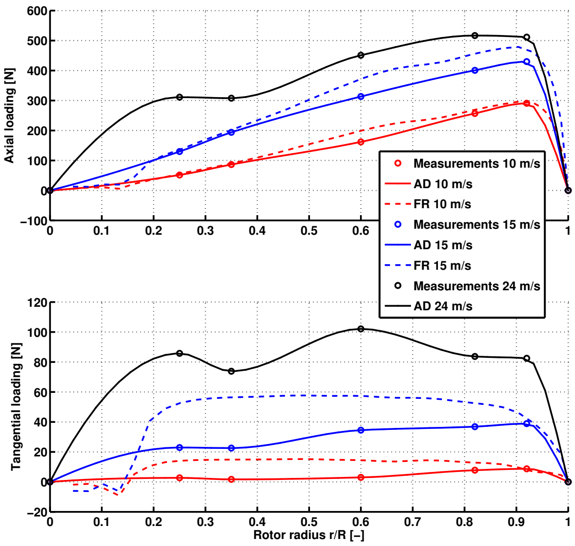

Figure 6: Description of the different wind turbine blade loadings. The Actuator Disc (AD) loadings are splined from the measurements points, while the Full Rotor (FR) computations loadings are estimated from the simulation results.

and a steady state solution. The transient solution is run with a time step of $\Delta t = 0.01$ sec, for 2000 iterations using 6 subiterations, which takes about 16h on 100 CPUs. The 2000 iterations on the steady state computation only takes 2-3 hours on 100 CPUs.

3 Results

3.1 Runs

With the different wind turbine models and types of mesh, 7 different types of runs are calculated at the 3 different wind speeds of the experiment (10, 15 and 24 m/s).

- Wind tunnel mesh without wind turbine steady state (Tunnel).
- Actuator disc model with wind tunnel steady state (AD-WT).
- Actuator disc model with wind tunnel without breathing slot steady state (AD-WT-noSlot).
- Actuator disc model without wind tunnel steady state (AD-noWT).
- Actuator disc model with wind tunnel unsteady DES (AD-DES).
- Full rotor computation with wind tunnel unsteady RANS (FR-WT).
- Full rotor computation without wind tunnel unsteady RANS transient (FR-noWT).

3.2 Streamwise Sections

Fig.7 presents the axial velocity in an horizontal line passing through the wind tunnel, without turbine, at hub height and $z/D = 0.33$ for various inlet velocity.

Fig.8 shows the axial velocity in an horizontal line passing through the wind tunnel at hub height and $z/D = 0.82132$ for the different wind turbine models, with and without the wind tunnel, for different inlet wind speed and compare them with the relevant wind speed measurements.

Fig.9 presents a comparison between different steady state actuator disc runs with different kind of meshes (without wind tunnel, and win tunnel with and without breathing slots).

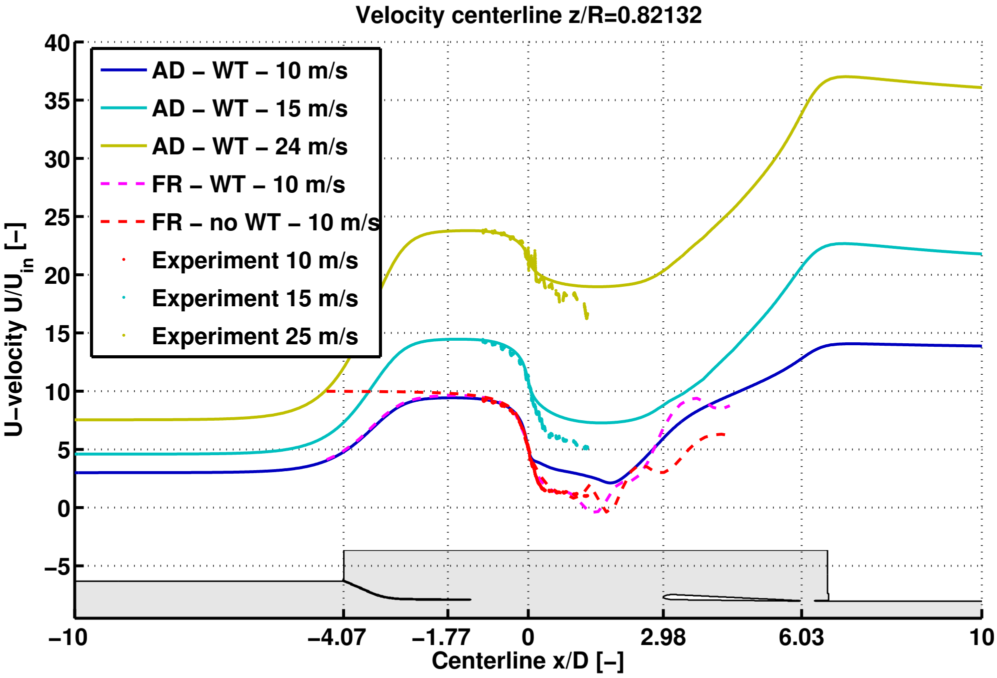

Figure 8: Comparison of different runs with respective measurements. With wind tunnel (WT) and without (no WT). With a steady state actuator disc (AD) and with an unsteady full rotor computation (FR).

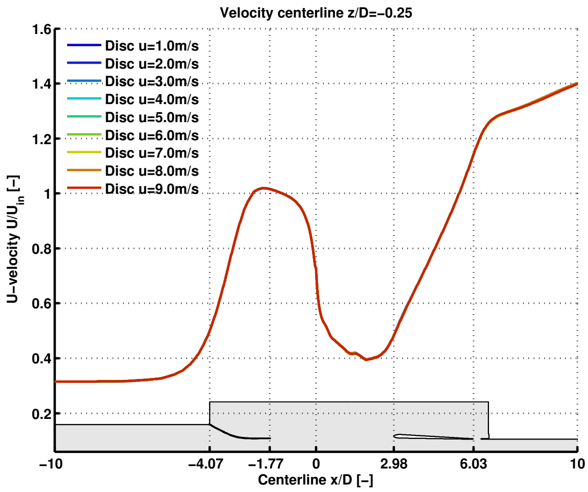

Figure 7: Wind tunnel with wind turbine of constant C_T at different wind speeds, collapsing when normalized. The wind speed indicated is the inflow wind speed at the inlet boundary. They are normalized with a constant ratio that would give unity at the wind turbine position, when no wind turbine is present.

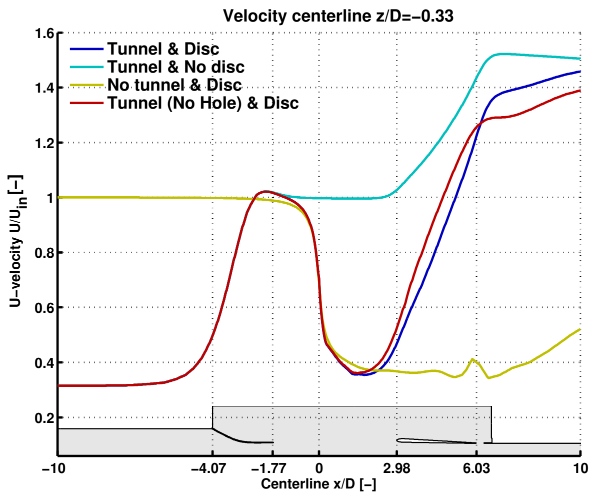

Figure 9: Comparison of different steady state actuator disc runs with respective measurements. With and without wind tunnel. With the 'breathing slots' and without (no hole)

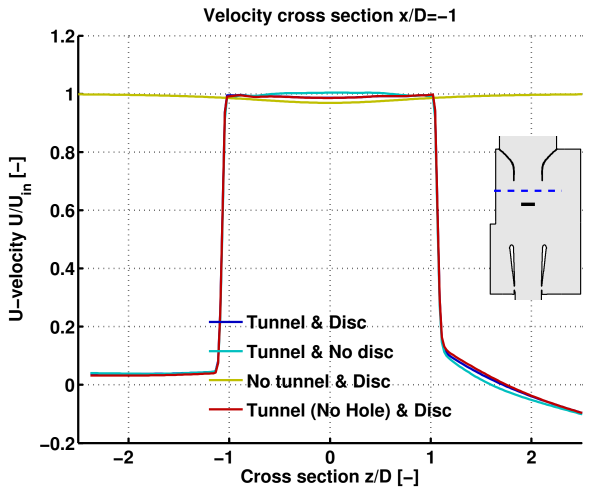

Figure 10: Transverse sections at different position upstream and downstream of the wind turbine from different types of simulations.

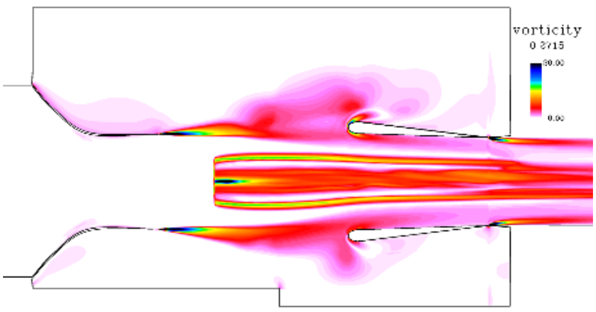

Figure 11: Actuator disc simulation of the MEX-ICO rotor (AD-WT). Vorticity colour contour in an horizontal plane at hub height.

3.3 Transverse Sections

Fig.10 shows the axial velocity along transverse sections at different positions downstream and upstream of the wind turbine (animated only in the digital version), including regions of perturbed flow. Different steady-state actuator disc simulations are presented: actuator disc with and without wind tunnel, actuator disc with a wind tunnel without breathing slots (no hole) and a simulation with a wind tunnel without actuator disct.

3.4 Contourlines

Fig.11 illustrates the vorticity contouts at hub height of a steady state actuator disc model with an inflow wind speed of 10 m/s.

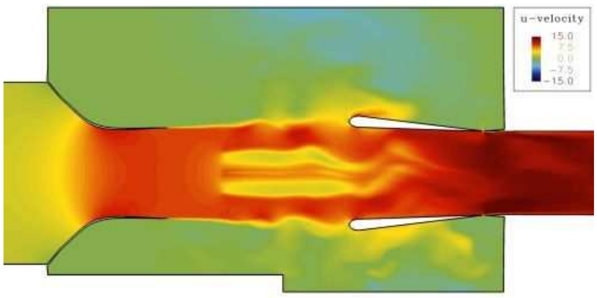

Figure 12: Actuator disc simulation of the MEX-ICO rotor. Axial velocity colour contour on a horizontal plane at hub height. Frames from the DES animation [11].

3.5 DES animation

A video of the unsteady animation (AD-DES) is available online [11]. An extract of it is also visible in the digital version of this article (Fig. 12).

4 Discussion

4.1 Reynolds Number independence

Fig.7 shows that the wind tunnel simulation is Reynolds Number independent. This shows that the jet development is not dependent of the inflow velocity. However, this mesh has a slip boundary condition on the wall, and therefore no boundary layer is developing. A mesh with a no-slip boundary condition might not be Reynolds number independent.

4.2 Flow Asymmetry

The horizontal asymmetry of the wind tunnel geometry (visible in e.g. Fig.1) seems to generate a wider recirculation zone on one side than on the other. This effect could explain why the wake entering the collector seems to be bended in Fig.11. It could also explain some lateral forces recorded on the wind turbine support structure.

4.3 Wind Tunnel Perturbations

The difference between the actuator disc simulations with and without wind tunnel seem to indicate that the wind tunnel collector can influence the wake measurements as soon as 1.5 rotor diameter downstream (see Fig.9-10). Similarly, the nozzle has an influence on the flow that cannot be ignore more than 1 rotor diameter upstream. Those observations are also visible while looking at the full rotor computations, Fig.8.

4.4 Breathing Slots Effect

From analyzing the results presented in Fig.9 and 10, the 'breathing slots' do not seem to have a significant effect in the region where the wind tunnel does not affect the flow ($x/D \in [-1, 1.5]$).

4.5 Jet Oscillation Effect

In the DES animations [11] there is a clear oscillation of the jet interface going in and out of the collector lips. These oscillations seem to have a significant effect on the wake dynamics (see also Fig.12). Nonetheless, while looking at the full rotor computation unsteady-RANS animation, this jet interface was not oscillating. The difference between the two simulations is that the unsteady-RANS allows a build up of the eddy-viscosity and the turbulence at the jet interface that could damp and account for those oscillations. In the DES simulations, there is a limit put on the turbulent length-scale size that effectively prevent an increase of eddy-viscosity. Nonetheless, it remains unclear if those oscillations did actually appear in the experiments and if they indeed had such a significant impact on the wake dynamics. More work needs to be done on this issue to answer this question.

4.6 Blade Loading and Flow Features

The flow characteristics found with the actuator disc model, based on the forces from the measurements, do not give satisfying results in comparison with the measurements. They systematically underpredict the wake deficit in comparison with both the measurements and the full rotor computations. This seems to indicate that the loadings estimated from the pressure sensors are not large enough to obtain the measured velocity deficits. This tends to agree with the results of Bechmann et al. [3] that indicates that the full rotor computations obtain significantly higher loadings (see also Fig.6).
The full rotor computation carried out with and without the wind tunnel give very close results in the region of comparison. This furthermore indicates that the wind tunnel effect cannot explain the mismatch between the forces measured on the blade and the axial velocity measurements.

5 Conclusion

The open wind tunnel of the MEXICO experiment was successfully modelled in CFD using two types of wind turbine models (Full rotor computation and actuator disc).
The results show that the effect of the wind tunnel over the region of comparison in the wake should not be significant. Similarly, the breathing slots are not found to have a significant influence in the region of interest.
However the DES analysis showed that there could be an oscillation of the wind tunnel jet interface that could potentially create a significant oscillation of the wake. It is unclear if this effect can be observed in the MEXICO measurements and if they had an impact on the quality of the experiment. More work should be focussed on this question, as it raises a potential issue with future open wind tunnel experiments of wind turbine wakes.
Finally there seems to be a mismatch between the blade loadings measured and the axial velocity measurements. Both the full rotor computation and the actuator disc model cannot match both results at the same time satisfyingly. This could potentially indicate an under estimation of the blade loadings.

Acknowledgement

The authors are grateful for the IEA project MEXNEX and the DSF Flow center for financing this work, DNW for providing the wind tunnel geometry and J.G. Schepers, K. Boorsma and H. Snel from ECN and for providing the wind turbine measurements.

References

[1] MEXICO experiment web site. http://www.mexnext.org/resultsstatus.

[2] A. Bechmann. *Large-Eddy Simulation of Atmospheric Flow over Complex Terrain.* PhD thesis, DTU-MEK, Denmark, 2007.

[3] A. Bechmann, N. N. Sørensen, and F. Zahle. CFD Simulation of the MEXICO Rotor Wake. *Wind Energy (in revision).*

[4] R. I. Issa. Solution of the implicitly discretised fluid flow equations by operator-splitting. *Journal of Computational Physics*, 62(1):40–65, January 1986.

[5] B. P. Leonard. A stable and accurate convective modelling procedure based on quadratic upstream interpolation. *Comp. Meth. in Appl. Mech. and Engrng.*, 19:59–98, 1979.

[6] F. R. Menter. Zonal two equation k- turbulence models for aerodynamic flows. *AIAA Journal*, (93-2906), 1993.

[7] J. A. Michelsen. Basis3D - a platform for development of multiblock PDE solvers. Technical report AFM 92-05, Technical University of Denmark, Lyngby, 1992.

[8] S. V. Patankar and D. B. Spalding. A calculation procedure for heat, mass and momentum transfer in three-dimensional parabolic flows. *Int. J. Heat Mass Transfer*, 15:1787–1972, 1972.

[9] P.-E. Réthoré. *Wind Turbine Wake in Atmospheric Turbulence*. PhD thesis, Aalborg University - Risø DTU, October 2009. [PDF].

[10] P.-E. Réthoré and N. N. Sørensen. Actuator disc model using a modified Rhie-Chow/SIMPLE pressure correction algorithm. *EWEC Brussels*, 2008. [PDF].

[11] P.-E. Réthoré, N. N. Sørensen, and H. A. Madsen. Wind tunnel model of the mexico experiment. *Wind Energy Research*, 2010. http://windenergyresearch.org/?p=81.

[12] P.-E. Réthoré, N. N. Sørensen, and F. Zahle. Validation of an Actuator Disc Model. *EWEC Warsaw*, 2010.

[13] J. G. Schepers and H. Snel. Model experiments in controlled conditions, final report. Technical report, Energy Research Center of the Netherlands, ECN. ECN-E-07-042, 2007. [PDF].

[14] N. N. Sørensen. *General Purpose Flow Solver Applied to Flow over Hills*. PhD thesis, Technical University of Denmark, 1994.

[15] F. Zahle. *Wind Turbine Aerodynamics Using an Incompressible Overset Grid Method*. PhD thesis, Imperial College, London, 2007.